

APPLICATION OF FRACTURE MECHANICS. METHODOLOGY TO ASSESS THE INTEGRITY OF REELED PIPES

H. Ernst

Center for Industrial Research & Development, Tenaris Group, Simini 250 – 2804 Campana, Argentina, e-mail: hernst@tenaris.com

ABSTRACT

The reeling process is one of the most important methods for offshore installations of linepipes. Pipe segments are welded onshore and subsequently bent over a cylindrical rigid surface (reel) in a laying vessel. The pipe is significantly cyclically strained.

Due to the severe loading cycles suffered by the pipes, it is necessary an adequate methodology to assess the integrity of these components.

Current recommended methodologies were not specifically developed for reeling situations, If are straightforward applied unreliable results can be obtained.

In the current work, the points that need to be resolved before extending the methods for assessing reeling situations are clearly identified. Theoretical models to describe the crack driving force evolution and the material fracture resistance behavior through strain cycles are proposed. As a result a methodology to assess the integrity of pipes subjected to a single reeling cycle is developed.

The case where several reeling cycles are applied is considered. In addition to the fracture mechanics methodology, a fatigue crack growth formulation controlled by ΔJ parameter is proposed. This formulation accounts for the crack growth produced during subsequent reeling cycles.

In addition, a probabilistic fracture mechanics approach is included. This procedure takes into account the statistical distributions of the material properties and pipe geometry, using the Monte Carlo method. Two-parameter Weibull distributions were used to model the variability of the input parameters.

Fatigue and fracture experimental programs were developed. Monotonic and cyclic fracture mechanic tests were performed on single edge notch in tension (SENT) specimens.

As result, a general methodology for assessing the integrity of pipes under reeling condition was proposed.

1. INTRODUCTION

1.1 Reeling of Pipes

Reeling is a fast and efficient method often used to install pipelines offshore. This method consists of welding onshore pipe segments that are reeled onto a spool and later transported out to the sea. In a standard reeling cycle, the welded pipes are reeled onto a drum, reeled off, aligned and straightened. During installation, the pipes are significantly cyclically strained and plastic deformation is introduced.

Reeling has many advantages because the welding, coating and inspection are carried out onshore. Particular situations may arise (extreme weather conditions, etc.) where the deployed line must be retrieved to the reel. In these situations, the pipe is subjected to multiple reeling cycles. In this work, the reeling cycle is considered as constituted by two deformation steps, and each step by a loading branch followed by an unloading branch.

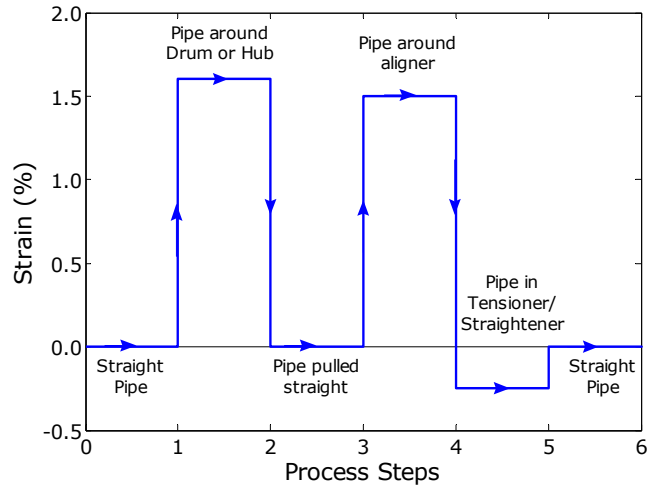


Fig 1. Typical Strain History during Reeling Operation

1.2 Structural Integrity Analysis

A structural integrity analysis is a method that gives the defect acceptability levels for a particular structure. This analysis must be carried out in order to confirm that failure from possible defects will not occur. Two of the main failure mechanisms are fracture and plastic collapse.

Failure by plastic collapse takes place when a critical value of plastic deformation is reached in the structure's remaining ligament and the defect is considered as lacking resistant area. The load causing plastic collapse depends on material mechanical properties and tube and defect geometry.

Fracture involves stable crack growth by ductile tearing followed by unstable fracture. Once the crack starts to extend, crack propagation may occur extremely fast. For fracture to occur, a detrimental combination of applied stress, crack dimension and the material fracture toughness is required.

For materials that fracture in an elastic-plastic way, the fracture parameters needed to perform a integrity analysis are: the applied J (or crack driving force) and the material J (or material fracture toughness).

1.2.1 Crack Driving Force

Crack driving force, or applied J (J_{app}), is calculated using equations involving the applied load, P (or remotely applied strain, ϵ_{app}), the defect size, a, and the geometry of the structure.

The J_{app} can be expressed as the addition of elastic, J_{ee} , and a plastic, J_{pl} contributions [1]:

$$J_{app} = J_{app}(P, a) = J_{ee} + J_{pl} \quad (1)$$

Where J_{ee} is:

$$J_{ee} = \frac{(K_{ae}(a + r_y))^2}{E} \quad (2)$$

According to EPRI [2], for materials that follow the Ramberg-Osgood equation, J_{pl} is:

$$J_{pl} = \frac{\alpha a Y^2}{E} \cdot \left(1 - \frac{a}{t}\right) \cdot h_1 \cdot \left(\frac{P}{P_0}\right)^{n+1} \quad (3)$$

Where:

$$h_1 = h_1\left(\frac{a}{t}, n\right) \quad (4)$$

The parameters are:

- t = Thickness
- r_y = Crack tip plastic zone radius
- P_0 = Limit load
- J_{ee} = Elastic part of the driving force corrected by small scale yielding
- J_{pl} = Plastic part of the driving force
- K_{ae} = Effective Stress Intensity Factor
- E = Elastic Modulus
- n = Hardening exponent (Ramberg-Osgood exponent)
- α = Material constant (Ramberg-Osgood coefficient)
- Y = Yield strength
- ϵ_0 = Yield strain (Y/E)

1.2.2 Material Fracture Toughness

Some materials exhibit a high toughness and do not fail catastrophically immediately after crack initiation. In these cases the material fracture resistance parameter, J_{mat} , may be expressed as a function of crack growth, Δa . This curve is obtained experimentally.

$$J_{mat} = J_{mat}(\Delta a) \quad (5)$$

1.2.3 Fracture Criterion

Failure by fracture occurs if the crack driving force, J_{appl} , is equal or greater than the fracture toughness, see Fig. 2. The condition for crack initiation is attained when the J_{appl} exceeds a critical value J_{IC} :

$$J_{appl} = J_{IC} \quad (6)$$

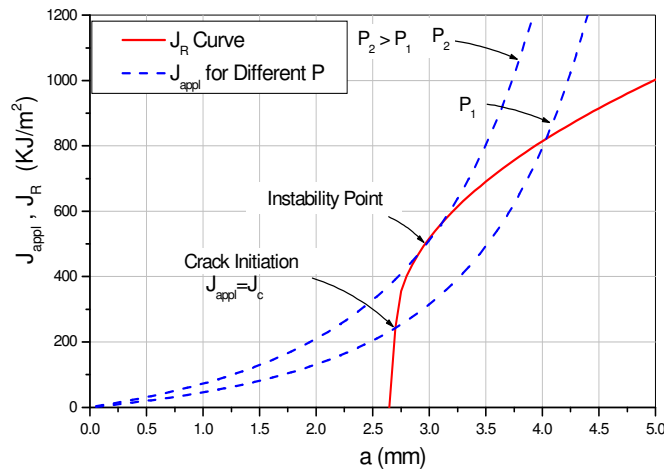


Fig. 2. Fracture Criterion

After some amount of stable crack extension, the crack growth process may become unstable. This event depends on material properties, geometry and loading conditions. Earlier works [3, 4, 5] showed that the instability condition occurs when the driving force curve, $J_{appl}(a, P)$, is tangent to the $J_{mat}(\Delta a)$ curve. Figure 2 shows the instability condition:

$$\left(\frac{dJ}{da} \right)_{appl} = \left(\frac{dJ}{da} \right)_{mat} \quad (7)$$

1.3 Statistical Distributions

If all the parameters needed to perform a structural integrity assessment are fixed, a deterministic analysis can be straightforward performed.

Nevertheless, material properties, as well as geometric parameters usually have a specific statistical distribution. This variability will produce different results in the deterministic assessment, depending on

the value of the parameters used. So, choosing a single set of values for the parameters of interest does not show the real distribution of the output parameters.

1.4 Problems to be Addressed in the Assessment of Reeled Pipes

The fracture mechanics parameters previously mentioned were developed for cases where structures are monotonically loaded. It is not clear how these parameters can be used for cases where cyclic deformation takes place. In fact today recommended practice [6] assumes that: 1) fracture mechanics parameters can be calculated using the equations developed for monotonically increasing load conditions, i.e. ignoring the effects of plastic unloading, and 2) the amount of crack growth that takes place in each cycle responds to a resistance curve description that is shifted to the new initial crack length every time, i.e. ignoring previous history. As a result then, the following points need to be addressed before applying an assessment methodology to a pipe subjected to reeling:

i) Stress-strain relationship: After stress reversal(s) the stress-strain relationship is not unique. It is necessary to know the specific stress - strain relationship throughout the full strain excursion.

ii) Applied fracture mechanic parameters: For monotonically increasing load cases, it is known that $J_{\text{appl}}(a, P) = J_{\text{appl}}(a, v)$, assuming as valid the functionality $v = v(P, a)$.

When unloading and reloading take place, the applied fracture mechanics parameters (J_{appl} , $CTOD_{\text{appl}}$) are not clearly defined, i.e. $J_{\text{appl}}(a, P) \neq J_{\text{appl}}(a, v)$. It is not clear what stress have to be considered to determine the J_{appl} or $CTOD$ for a given deformation.

ii) R-curve: The material fracture mechanics parameters (J_{mat} , $CTOD_{\text{mat}}$) evolution through the strain cycles is unknown, i.e. when the component is loaded, unloaded and reloaded, it is not known if the value of J_{IC} remains at the same level or if is shifted to a new value.

iv) Multiple Cycles: The case of several loading cycles must be studied probably including a fatigue formulation in the methodology.

v) Probabilistic: Deterministic analyzes gives unrealistic results due to the variability of the involved parameters, and then a probabilistic approach should be developed.

In the following sections, the last four items will be addressed in detail.

For the problem of stress-strain relationship, the cyclic relation can be obtained experimentally for the specific material, or theoretically using a model that describes the stress response to strain cycles. A simple example of a theoretical relation is presented in the appendix 1.

2. ASSESSMENT FOR REELED PIPES

The most accepted methodology to assess critical defect sizes in welded structures is based on British Standard 7910 [7]. For applications where high cyclic plastic deformations take place, such as reeling installation, specific corrections [6, 8, 9] to BS 7910 have to be done.

As was mentioned, currently recommended methodology considers that every positive strain increment is active in terms of crack driving force, and material fracture toughness, J_{mat} , is taken as "history independent" for each strain increment. This means that every strain increment contributes to crack extension, independently of previous load conditions.

Based on these facts, it seems to be necessary to adequately describe the crack driving force evolution and the material fracture resistance behavior through strain cycles [10].

2.1 Crack Driving Force For Complex Strain History

When cyclic deformation is considered the applied fracture mechanics parameters are not clearly defined. For this reason, the present section will be focus on addressing the problem of the evolution of the applied fracture mechanics parameters through strain cycles.

A model based on the Rice analysis of reverse plasticity [11] is proposed to describe the evolution of the applied fracture mechanic parameter through the strain cycles.

Stress, strain and displacement results from the Rice model may be represented in the general form:

$$\sigma_{ij} = Y \Sigma_{ij}(r/a, \theta, P/Y) \quad (8)$$

$$\varepsilon_{ij} = \varepsilon_0 E_{ij} \Sigma_{ij}(r/a, \theta, P/Y) \quad (9)$$

$$\mu_i = \varepsilon_0 a U_i \Sigma_{ij}(r/a, \theta, P/Y) \quad (10)$$

for monotonic loadings, where r , θ are polar coordinates centered at the crack tip, P is a remote applied load, Y and ε_0 are a representative yield stress and strain, and Σ_{ij} , E_{ij} and U_i are dimensionless functions of their arguments, reversing sign with sign reversal of P .

The stress, strain and displacement after unloading are $\sigma_{ij} - \Delta\sigma_{ij}$, $\varepsilon_{ij} - \Delta\varepsilon_{ij}$, $\mu_{ij} - \Delta\mu_{ij}$, respectively where the change in value of the field variables, due to load reduction from P to $P - \Delta P$, is given by:

$$\Delta\sigma_{ij} = 2\sigma_0 \Sigma_{ij}(r/a, \theta, \Delta P / 2\sigma_0) \quad (11)$$

$$\Delta\varepsilon_{ij} = 2\varepsilon_0 E_{ij} \Sigma_{ij}(r/a, \theta, \Delta P / 2\sigma_0) \quad (12)$$

$$\Delta\mu_i = 2\varepsilon_0 a U_i \Sigma_{ij}(r/a, \theta, \Delta P / 2\sigma_0) \quad (13)$$

An incremental method is used to calculate CTOD (crack face displacement at a single point) evolution. No attempt was made to describe stress-strain fields ahead of crack tip through a single parameter. Using Rice's model, the CTOD value, for a generic point X , (P, v) , beyond the stress reversal point A , is:

$$CTOD_X = CTOD_A + \delta CTOD_{AX} \quad (14)$$

Where $CTOD_A$ is the value of the CTOD at the reversal point A , and $\delta CTOD_{AX}$ is the change in CTOD value in going from point A to point X . The $\delta CTOD$ can be written as:

$$\delta CTOD = dn(Y', n) \delta J / Y' \quad (15)$$

Where δJ is calculated using the same functional dependence of J but replacing the stress by the stress increment and Y by Y' , which is the yield strength corresponding to that particular point.

If $J = J(\sigma, a, Y, \varepsilon_0, \alpha, n)$ then, $\delta J = J(\Delta\sigma, a, Y', \varepsilon_0', \alpha, n)$.

Specifically, referring to a typical test record, the value $\delta CTOD$ can be obtained taking the reversal point as origin, and the axis (P', v') , i.e. Load = $P - P_{rev}$ and displacement = $v - v_{rev}$.

$$\delta CTOD = CTOD(P - P_{rev}, a) \quad (16)$$

With $\delta CTOD < 0$ for $d\sigma/dt < 0$ and $\delta CTOD > 0$ for $d\sigma/dt > 0$, or using $\delta CTOD = dn(Y', n) \delta J / Y'$.

For the generic point $X1$, beyond A (loading + unloading):

$$CTOD_{X1} = CTOD_A + \delta CTOD_{AX1} \quad (17)$$

Where $(-\delta CTOD_{AX1})$ is the value of CTOD at load P_{X1} or displacement V_{X1} , referred to the new coordinate axes (P', v') . Defining:

$$P'_{X1} = P_{rev} - P_{X1} \quad (18)$$

And

$$v'_{X1} = v_{rev} - v_{X1} \quad (19)$$

So

$$-\delta CTOD_{AX1} = (-\delta J_{AX1}) / Y' \quad (20)$$

$$-\delta CTOD_{AX1} = J(P'_{X1}, a) / Y' \quad (21)$$

$$-\delta CTOD_{AX1} = [K^2/E (P'_{X1}) + (\eta/bB)U_p(P'_{X1}, v'_{X1})] / Y' \quad (22)$$

η_p = Dimensionless function of the geometry

U_p = Plastic part of the area under the load vs. crack mouth opening displacement (CMOD)

B = Width of the specimen.

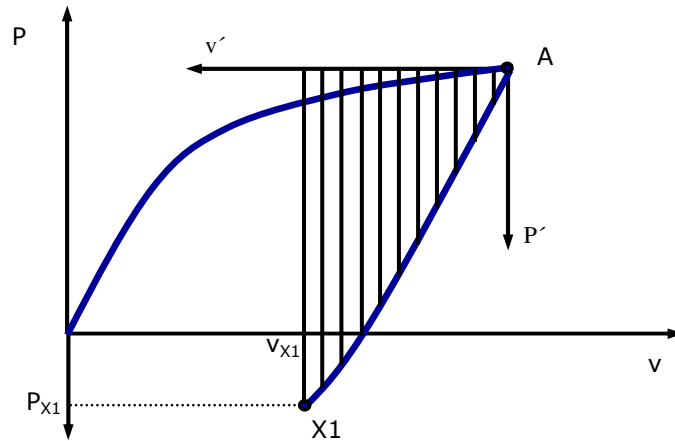


Fig. 3. Schematic unloading point and new coordinate axis (P' , v').

For a generic point X_2 , see Fig. 4, beyond a second reversal point B (loading + unloading + reloading):

$$CTOD_{X_2} = CTOD_B + \delta CTOD_{BX_2} \quad (23)$$

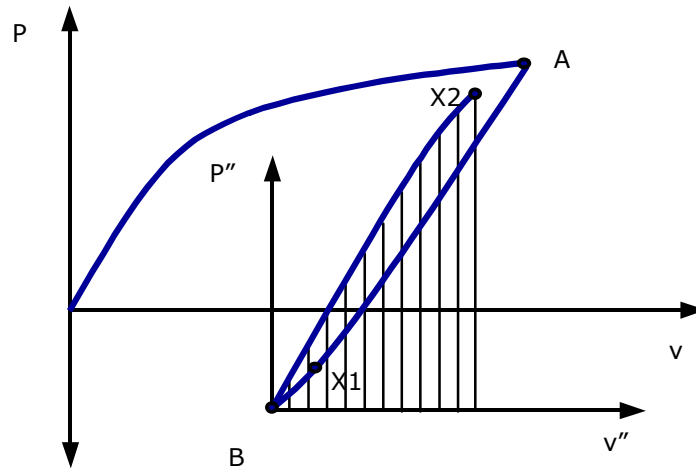


Fig. 4. Schematic reloading point and new coordinate axis (P'' , v'').

Defining:

$$P''_{X_2} = P_{X_2} - P_{rev} \quad (24)$$

$$v''_{X_2} = v_{X_2} - v_{rev} \quad (25)$$

So:

$$\delta CTOD_{BX_2} = (\delta J_{BX_2})/Y' \quad (26)$$

$$\delta CTOD_{BX_2} = J((P''_{X_2}), a)/Y' \quad (27)$$

$$\delta CTOD_{BX_2} = [K_2/E(P''_{X_2}) + (\eta/bB)U_p(P''_{X_2}, v''_{X_2})]/Y \quad (28)$$

This model is general for process where the deformation evolves cyclically. In this work the analysis was focused on the reeling process, but the methodology can be applied to other examples.

2.1.1 Experimental Work

An experimental program was carried out using single edge notch tension (SENT) specimens with fixed grips (no rotation at the ends) to study the effects of the strain history on the crack driving force parameter. The pipe studied was a $\varnothing 355.4$ mm x 22.2 mm WT SML 450 P (X65) and girth weld within DNV-OS-F101 requirements for reeling installation. The mechanical properties of Base and Weld Metal are summarized in the table 1.

Table 1. Mechanical Properties

	Yield Strength (MPa)	Tensile Strength (MPa)	Elongation (%)
Base Metal	476	565	32.6
Weld Metal	552	672	31.6

The specimens dimensions were: $W = 20$ mm, $B = 400$ mm, length = 360mm and $a_0/W = 0.225$. SENT specimens were chosen since they match the crack tip constraint of a pipe circumferentially cracked subjected to reeling. The specimens, in a clamped configuration, were subjected to different tension-compression cycles. Gauges were attached to the specimens to determine the Crack Tip Opening Displacement (CTOD), the Crack Mouth Opening Displacement (CMOD) and the remote deformation (ϵ).

Using the proposed model previously described, CTOD values were calculated along the test, based on the experimentally determined load vs. CMOD record.

The results obtained in the tests and comparisons with the prediction from the model are shown in Figs. 5-6, for samples of base and weld metal.

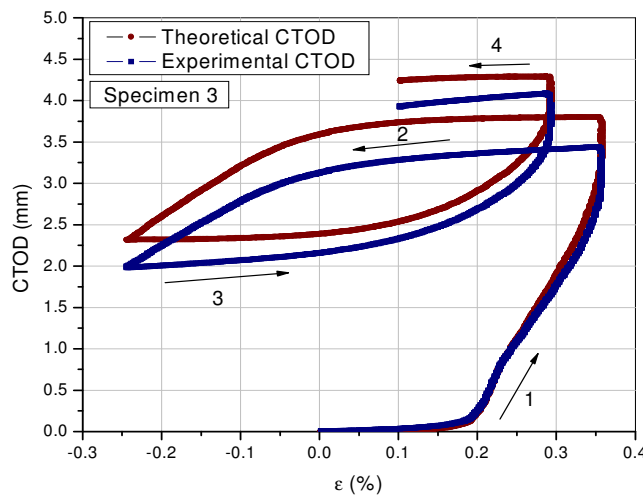


Fig. 5. Comparison Experimental / Theoretical CTOD. Base Metal.

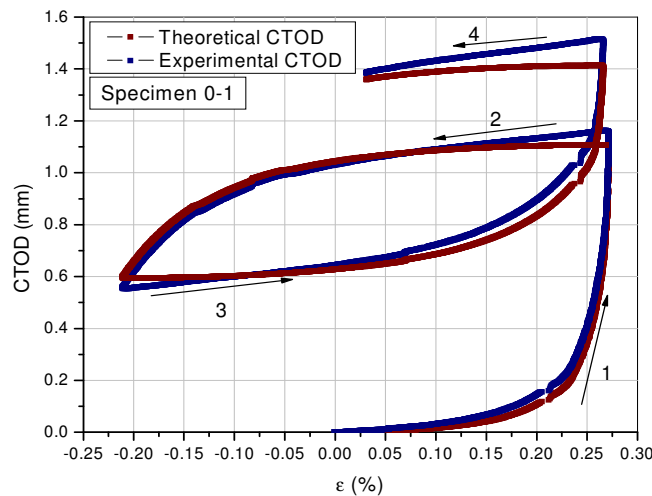


Fig. 6. Comparison Experimental / Theoretical CTOD. Weld Metal.

The proposed analytical model permits to determine CTOD as a function of strain history. Using this model the CTOD obtained in the unloading down to zero is approximately 95% of maximum CTOD reached in the loading. A very good agreement between predicted and measured CTOD values was obtained for the cases analyzed.

2.2 Resistance Curve Evolution

An experimental program was carried out using SENT specimens to study the material resistance curve evolution with complex strain history.

The specimens were subjected to different combination of cycles, they were broke open and the amount of crack growth, correspondent to each cycle, was measured.

The following extreme criteria were considered to describe the material resistance behavior through deformation cycles:

2.2.1 History Independent R Curve

The R curve is the same for all loading cycles. If crack extension takes place, then unloading + reloading, the curve is shifted towards the new initial crack length. In Fig. 7 it is shows schematically.

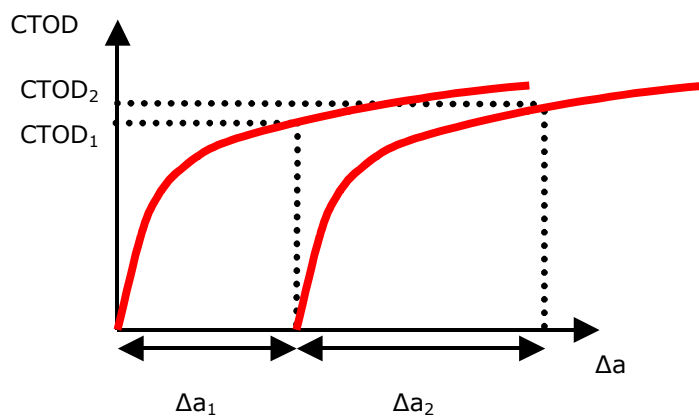


Fig. 7. History Independent R Curve

2.2.2 Material Memory R Curve

The R curve does not shift to a new origin. The CTOD value needed to cause further crack extension is the maximum reached in the previous cycle. In Fig. 8 could be observed the CTOD evolution following this criterion.

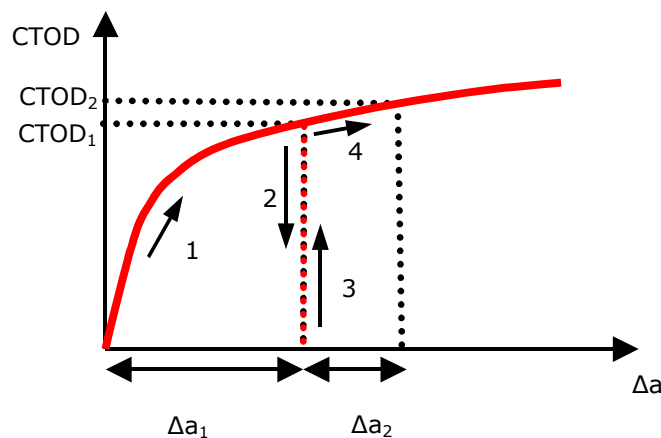


Fig. 8. Material Memory R Curve

The CTOD material resistance curves considering monotonic loading data (or single cycle data) are shown in Figs. 9-10. Cyclic data points were added. The points corresponding to the first cycle have a good agreement with the curve. For the second cycle data, two situations were considered: i) the final (second cycle) CTOD were plotted against Δa_2 which is the crack growth obtained in the second cycle

and ii) the final CTOD vs. Δa_{TOTAL} , that is the total crack growth (first cycle + second cycle). The figure shows that the last combination has good agreement with the curve.

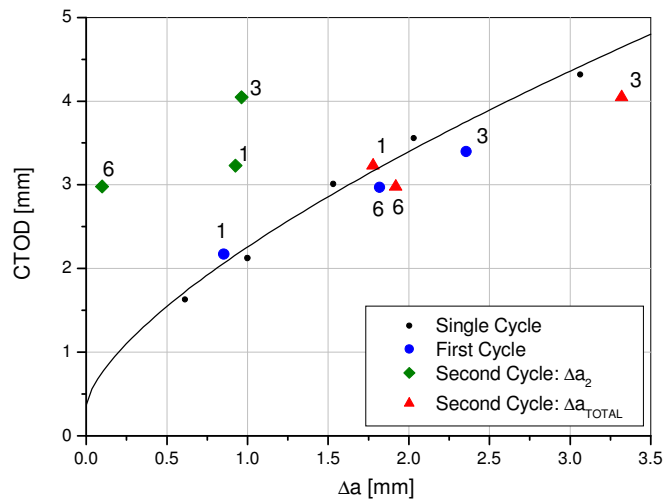


Fig. 9. CTOD vs. Δa with Cyclic Data - Base Metal

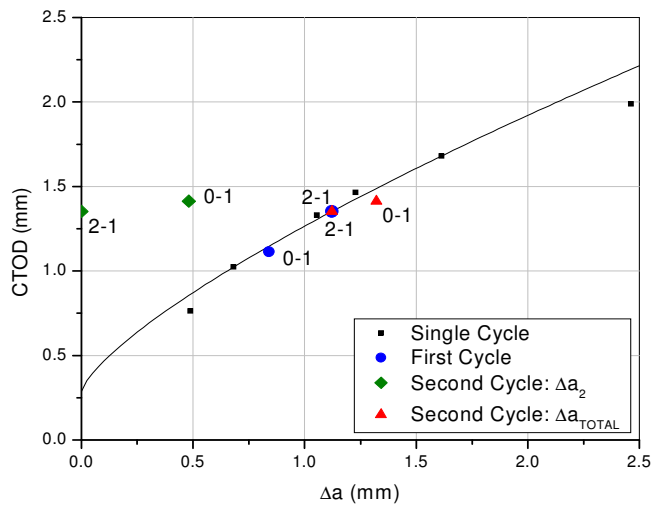


Fig. 10. CTOD vs. Δa with Cyclic Data - Weld Metal

Points obtained at the end of second cycles, in terms of CTOD, fell on the R curve (single cycle), provided Δa_{TOTAL} is used instead of Δa_2 . The whole amount of crack extension is accounted for by the R curve. No fatigue effects were observed for up to two deformation cycles. The material memory R curve criterion was validated by the experimental data, for up to two cycles. Presumably, if several more cycles are applied, fatigue effects need to be included.

3. MULTIPLE CYCLES

Crack extension produced by a single reeling cycle was estimated reducing the over conservativeness of current methods. In cases where multiples cycles are taken into account, fatigue formulations must be included in the model [12]. These formulations should account for fatigue crack growth under large yielding conditions.

Elastic-plastic fatigue crack growth was first studied by Dowling and Begley [13]. This work expands the fatigue formulation from linear elastic (ΔK) to large yielding conditions. The cyclic J-integral range (ΔJ) was taken as the fatigue crack growth driving force.

3.1 Elastic Plastic Fatigue Crack Growth (EP-FCG)

Under elastic-plastic conditions, fatigue crack growth is described by the use of the cyclic J-integral range (ΔJ) as driving force [13].

Based on deformation theory of plasticity, the applied fracture mechanics parameter (J or CTOD) can be evaluated using the final value of load (or displacement, v).

The driving force is obtained as the addition of two contributions, as shown in eq. 29. And ΔJ can be derived as:

$$\Delta J = \Delta J_{ee} + \Delta J_{pl} \quad (29)$$

ΔJ is not a difference of the J's, calculated with monotonic loading formulas, at maximum and minimum loads, i.e. $\Delta J \neq J(a, P_{max}) - J(a, P_{min})$. Instead, ΔJ is a single-valued function of the load or displacement increments (ΔP or Δv).

The elastic contribution, based on elastic fracture mechanics, is:

$$\Delta J_{ee} = \frac{(\Delta K_{ae(a+r_y)})^2}{E} \quad (30)$$

Where ΔK_{ae} is the effective alternating stress intensity factor

The plastic component (ΔJ_{pl}) can be determined by considering the P-v curve, see Fig. 11.

For a specimen with thickness B and uncracked ligament b, which is cyclically loaded between the loads P_{min} and P_{max} , and the load line displacements v_{min} and v_{max} , ΔJ_{pl} is calculated using the equation (31). η is a dimensionless function of the geometry.

$$\Delta J_{pl} = \frac{\eta}{B.b} \cdot \int_0^{\Delta v_{pl}} \Delta P \cdot d(\Delta v_{pl}) = \frac{\eta}{B.b} \cdot \int_{v_{min}}^{v_{max}} (P(v) - P_{min}) \cdot dv_{pl} \quad (31)$$

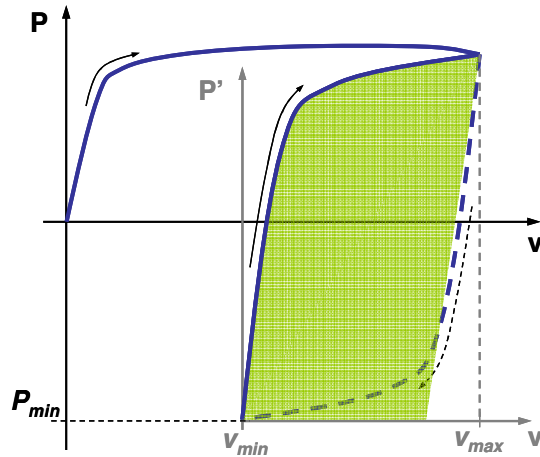


Fig. 11. Scheme of integration limits of ΔJ_{pl} based on P-v

3.2 Elastic-Plastic Fatigue Law

Once ΔJ is determined, fatigue crack growth behavior can be obtained extrapolating from linear-elastic (LE) range to elastic-plastic (EP) regime the following expression:

$$\frac{da}{dN} = C \cdot \Delta K^z \quad (32)$$

Where C and z are materials constants.

Combining equations (30) and (32), the EP-FCG can be easily correlated with ΔJ based on linear elastic formulations. The power law in equation (32) is now rewritten as:

$$\frac{da}{dN} = C' \cdot \Delta J^{z'} \quad (33)$$

Where,

$$C' = C \cdot E^{\frac{z'}{2}} \quad (34)$$

$$z' = \frac{z}{2} \quad (35)$$

Using equation (33), the fatigue crack growth for cyclic plastic loading can be determined.

3.3 Closure Correction

The ΔJ obtained from equations (30) and (31) is a nominal value that will be identified as ΔJ_{nom} . Fatigue crack growth is also dependent on the applied stress ratio ($R=P_{max}/P_{min}$). This dependence may be significantly reduced if crack closure correction concept is introduced [13, 14, 15, 16], obtaining more accurate results [13, 14, 15].

The closure effect assumes that during a part of the load cycle the crack surfaces come into contact and the crack closes. In this stage, the specimen behaves as an uncracked body and consequently there is no crack growth. In order to determine the effective load cycle an opening load (P_{op} , minimum load to open the crack) is considered.

To perform the closure correction based on P_{op} , the integral in equation (31) should be calculated between the opening and maximum limits (see fig. 12), as it is shown below:

$$\Delta J_{pl}^{eff} (P_{op}) = \frac{\eta}{B \cdot b} \cdot \int_{v_{op}}^{v_{max}} (P(v) - P_{op}) \cdot dv_{pl} \quad (36)$$

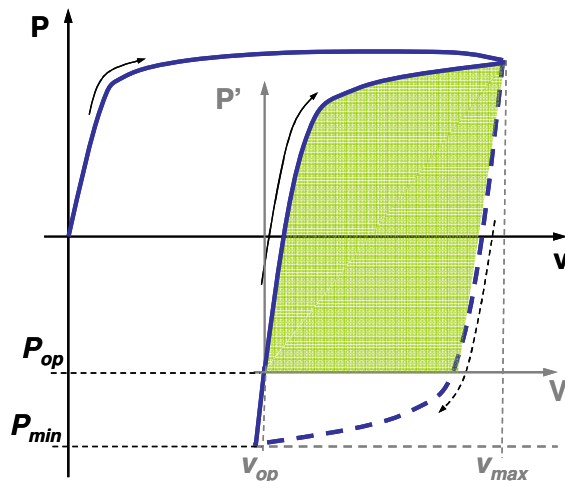


Fig. 12. Scheme of integration limits of ΔJ corrected by closure using P_{op}

3.4 Experimental Work

An experimental program was carried out in order to study the crack growth produced during multiple strain cycles.

Girth-welded joints from seamless steel pipes with OD 323.9 x wt 14.3 mm and OD 355.5 x wt 22.2 mm were used for the current analysis. Mechanical properties are shown in table 2.

Table 2. Mechanical Properties

Pipe	Yield Strength, Y [MPa]	Tensile Strength, T [MPa]
------	-------------------------	---------------------------

323.9 x 14.3	475	570
355.5 x 22.2	478	560

Single edge notched in tension (SENT) specimens were tested. The specimens, in a clamped configuration, were subjected to different tension-compression cycles. Examples are shown in fig. 13-14.

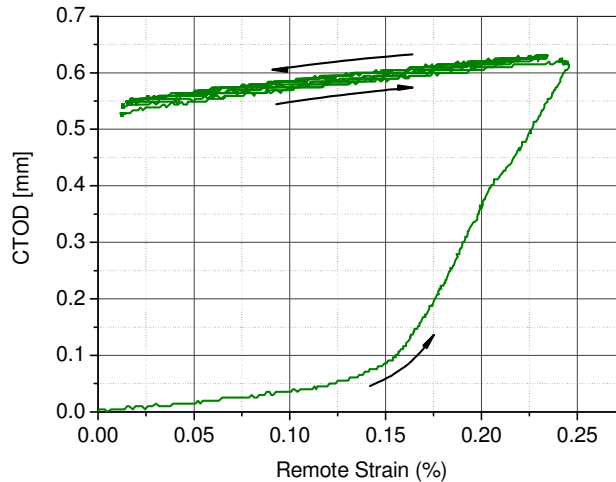


Fig. 13. Experimental CTOD-ε record for specimen 323.9x14.3-1

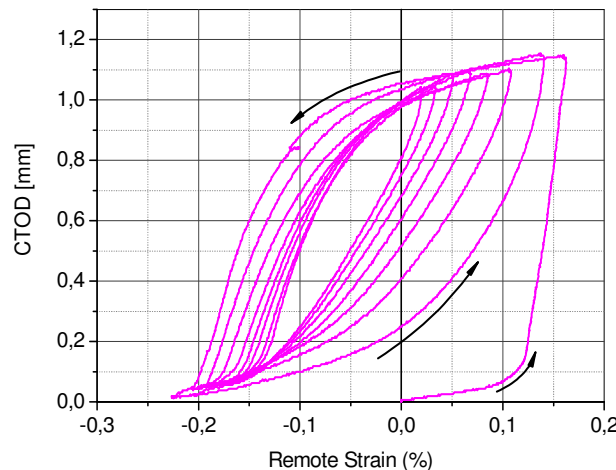


Fig. 14. Experimental CTOD-ε record for specimen 323.9x14.3-3

3.4.1 Fatigue Crack Extension

It is assumed that the total crack extension produced during repeated plastic strain cycles is the sum of two contributions. A tearing component produced only in the first deformation step (except that maximum strain previously reached be exceeded) and a fatigue component produced during subsequent ones. The tearing component is obtained by the R-curve following the material memory model, while the fatigue component may be determined as the total crack extension minus that produced by tearing.

$$\Delta a_{Fat} = \Delta a_{Tot} - \Delta a_{Tear} \quad (37)$$

Where,

Δa_{Tot} , is the total crack extension.

Δa_{Tear} , is the crack extension predicted by tearing.

Δa_{Fat} , is the fatigue crack extension produced during the subsequent deformation steps

It was assumed that the fatigue crack extension equally grows during the subsequent N-1 deformation steps (N is the total number of steps), therefore it can be considered that:

$$\frac{da}{dN} \approx \frac{\Delta a_{Fat}}{N-1} \quad (38)$$

So, the fatigue crack increment per cycle can be obtained from the experimental results.

3.4.2 Fatigue Laws

The law for air and $R > 0.5$ presented in British Standard 7910 [7] is considered to be precise enough to describe fatigue crack growth for this case. The law and the experimental points are presented in fig. 15.

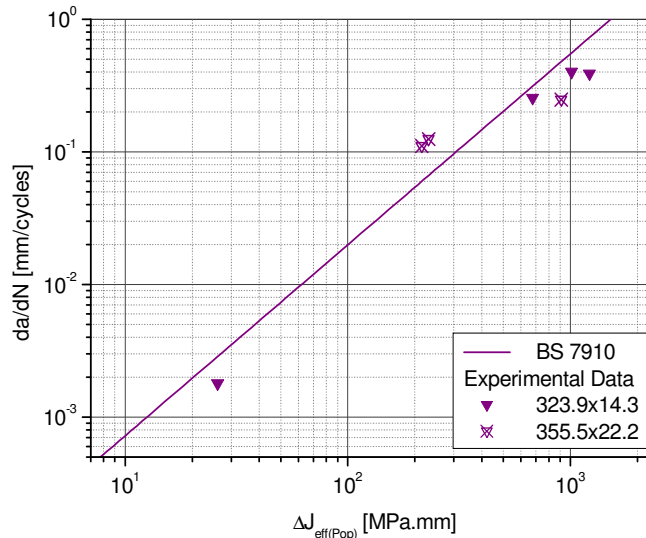


Fig. 15. Selected fatigue law and experimental results using closure correction by P_{op}

The selected fatigue law is presented in table 3 in terms of ΔK and ΔJ .

Table 3. Fatigue law coefficients

	ΔK [MPa.mm ^{1/2}]	ΔJ [MPa.mm]
n	2.88	1.44
C	5.86×10^{-13}	2.626×10^{-5}

4. PROBABILISTIC APPROACH

As the statistical distributions of the random variables involved in the assessment must be taken into account, a probabilistic fracture mechanics reliability analysis seems to be the most adequate approach.

4.1 Model

Based on fracture mechanic concepts and using the Monte Carlo method, a model was developed to incorporate the variability of material properties and pipe geometry in the analysis [17].

The Monte Carlo method basically consists of assigning random values, following a predetermined probability distribution, to some or all input variables involved, while keeping the rest deterministic. A set of values of all the variables is obtained and the problem is solved using the deterministic model. This procedure is repeated many times in order to obtain statistical results considering the distribution of the input variables.

Two-parameter Weibull distributions were used to model the variability of the random variables.

The main outputs of the computer model implemented are the statistical distribution of critical crack size and the cumulative probability (CP) of failure for a given crack size. The CP is defined as the probability of failure for a given defect size and assuming that this defect exists in the structure.

4.2 Weibull Function

Two-parameter Weibull probability density function was used to model the statistical distribution for each independent variable. Weibull function has the following expression:

$$f(x) = \frac{\gamma}{\lambda} \left(\frac{x}{\lambda} \right)^{\gamma-1} e^{-\left(\frac{x}{\lambda} \right)^\gamma} \quad (39)$$

Where λ and γ are the scale and shape parameters respectively. For the current case of interest, $\gamma > 1$, the probabilistic density function is bell shaped. The most important difference between Weibull and Normal functions is the fact that the Weibull is zero for $x \leq 0$, i.e. the probability of having a negative value of x is exactly zero.

4.3 Input Variables of the Model

The variables that were used in the model to perform the reliability analysis are mechanical properties, fatigue properties, material fracture toughness curve (J_{mat}) and crack driving force curve (J_{appl}).

The mechanical properties of the material are the yield strength, tensile strength and the Ramberg-Osgood parameters (n and α).

The variability in the fatigue properties is associated with the coefficient C (exponent z is kept fixed).

The material fracture toughness curve is a function of the crack growth (Δa), and its functional expression was taken as:

$$J_{mat}(\Delta a) = m + l \cdot \Delta a^x \quad (40)$$

Where x , l and m are material constants. This expression is in accordance with BS 7448 standard [18]. The crack driving force curve is a function of the pipe geometry: radius and thickness; the defect geometry: depth and length; the applied load and the material properties.

4.4 Program Outputs

As mentioned, the program finds the critical defect size for each set of values of the parameters and performs a statistical analysis of these results. The outputs are:

- Critical initial crack size distribution
- Final crack size distribution
- Amount of crack extension distribution
- Cumulative probability of failure: As was mentioned, is the failure probability for a tube having a given defect. The probability of existence of this defect is not considered.

5. PROPOSED ASSESSMENT METHODOLOGY FOR MULTIPLE REELING CYCLES

A methodology to assess the reliability of pipes subjected to multiple reeling cycles, taking into account the statistical distribution of the involved parameters, is proposed. The following assumptions must be considered:

- The first deformation step produces crack growth due to tearing mechanism. Further crack extension due to tearing will only be considered if subsequent deformation step exceeds the maximum deformation reached, according to material memory model.
- Each subsequent positive strain increment contributes to crack extension by fatigue in accordance to the selected fatigue law.
- The fatigue crack growth formulation should account for the effect of large plastic strain (elastic-plastic fatigue formulations). ΔJ corrected by P_{op} is considered as the effective driving force for fatigue crack growth.
- The final crack extension will be the linear addition of tearing and fatigue components (in accordance to [16]).
- Elastic-plastic fracture mechanics is used to define the critical condition to failure [3, 4, 5].
- No delay effects due to overloads are considered.
- Variability of the inputs parameters of both fracture and fatigue mechanisms are taken into account.

6. CASE STUDIED

The model was applied to a particular case of interest. A pipe with proposed fixed geometry and mechanical, toughness and fatigue properties distributions was analyzed. The properties were selected to represent a seamless pipe used as pipeline in oil industry. Tolerable defect limits were obtained for different probabilities levels of survival. A total of 1000 random of values were generated for each parameter. These random values followed a two-parameter Weibull distribution.

6.1 Geometry

A seamless steel pipe with OD 323.9mm x wt 14.23 mm was taken into account for the current analysis.

6.2 Mechanical Properties

Mean and standard deviations of the considered mechanical properties are summarized in Table 1.

Table 4. Mechanical Properties

	Mean	Standard Deviation
Yield Strength [MPa]	475	26
Tensile Strength [MPa]	570	28

6.3 Material Fracture Toughness - Resistance Curve

The resistance curve considered is a power law of three parameters [18]. The parameters of equation (40) are $m = 102$, $l = 723$ and $x = 0.68$. Standard deviations of 10% for each parameter were assumed.

6.4 Fatigue Law

The parameters chosen for the fatigue law given by equation (33) were obtained. The values of these parameters are presented in the following table:

Table 5. ΔJ [MPa.mm] Fatigue law coefficients

z	1.44
C	2.626×10^{-5}

6.5 Strain Cycles

The reeling cycle corresponds to reeling and unreeling unto a spool of radius of 8.2 m and a straightener with a radius of 55.8 m. The resultant applied strain sequence was: 1.98; -0.29; 1.98; -0.29; 0 %.

Tolerable defect size curves were obtained for other reeling cycles, which were composed of 1, 2, 4 and 8 repetitions of the previously defined applied strain sequence.

6.6 Critical Crack Size Distribution

Tolerable defect size curves were determined for crack aspect ratios (a/c) of 0.2, 0.4, 0.6 and 0.8.

Figure 16 shows an example case of critical initial defect size distribution, considering only one reeling cycle and a defect aspect ratio of 0.2.

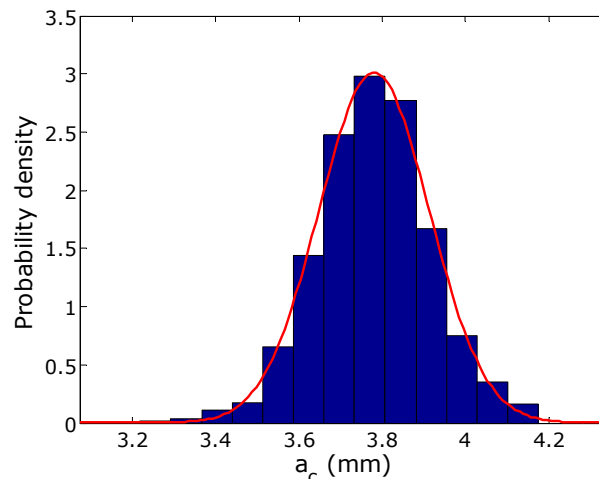


Fig. 16. Histogram of the critical defects obtained and a normal probability density function (red line)

6.5 Cumulative Probability of Failure

The cumulative probability of failure corresponding to the previous example of critical defect size distribution is presented in Figs. 17-18. In Fig. 18 the results are shown in a semi-logarithmic scale, to better appreciate the probability for smaller defects.

This probability is calculated assuming that the tube has in fact a given defect, a_c .

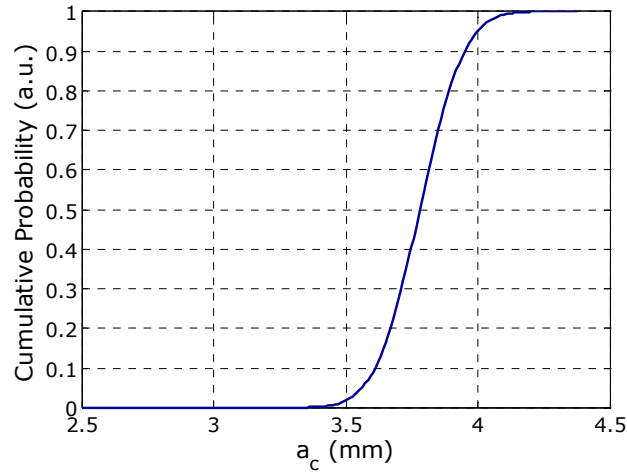


Fig. 17. Cumulative probability of failure.

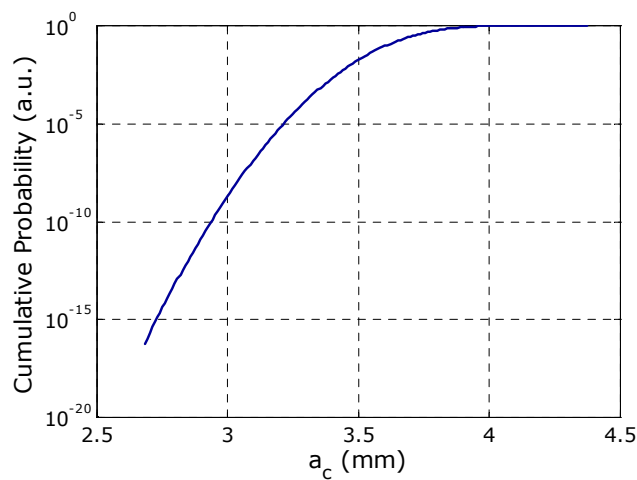


Fig. 18. Log-normal plot of the cumulative probability.

6.6 Tolerable Defect Size Curves

Tolerable defect size curves for different quantities of reeling cycles applied: 1, 2, 4 and 8 cycles are shown in figures 19-22. Each one of these cycles includes a laying and a retrieving of the pipe. For each one of these cases the curves of probability of survival of 50% and 95% are plotted. The probability of survival is defined as 100% less the probability of failure (in percentile).

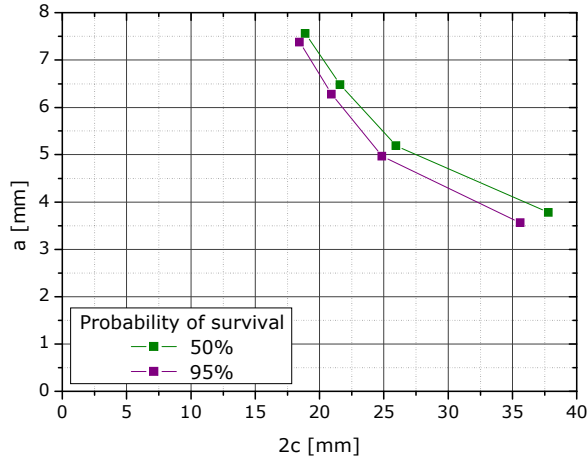


Fig. 19. Tolerable defect size (a vs. 2c) for different probabilities of survival and for only one reeling cycle.

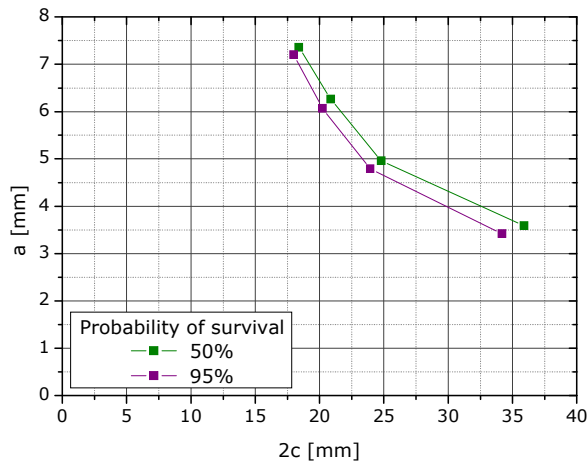


Fig. 20. Tolerable defect size (a vs. 2c) for different probabilities of survival and for two reeling cycles.

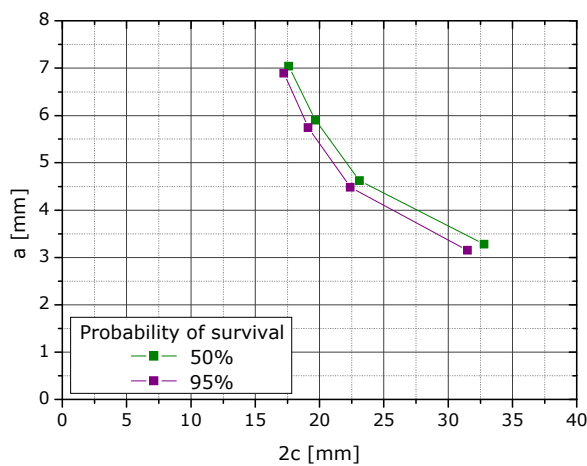


Fig. 21. Tolerable defect size (a vs. 2c) for different probabilities of survival and for four reeling cycles.

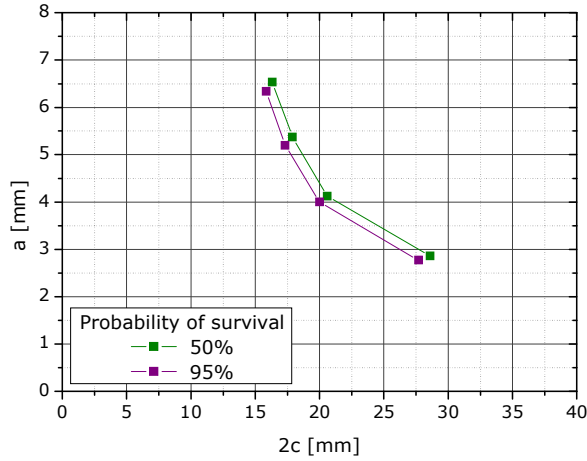


Fig. 22. Tolerable defect size (a vs. 2c) for different probabilities of survival and for eight reeling cycles.

Fig. 23 and 24 show tolerable defect curves for two different probabilities of survival: 50% and 95% respectively. The effect of the number of reeling cycles may be appreciated.

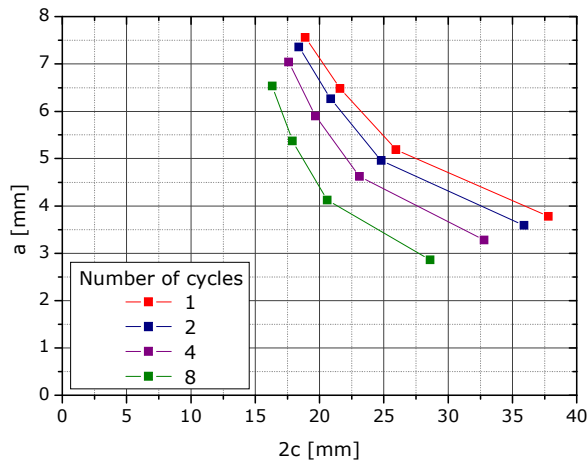


Fig. 23. Tolerable defect size (a vs. 2c) for a 50% probability of survival - Different number of cycles

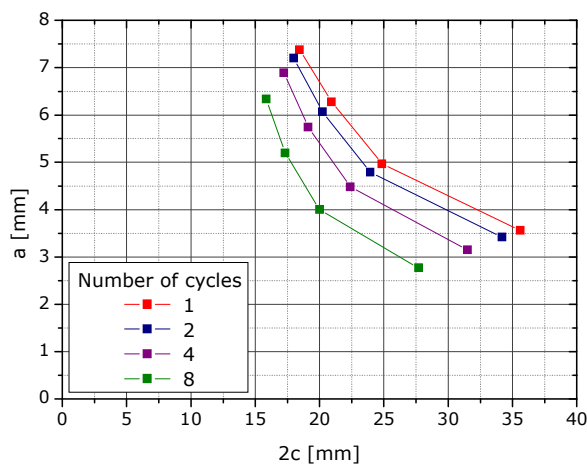


Fig. 24. Tolerable defect size (a vs. 2c) for a 95% probability of survival - Different number of cycles

The effects of the statistical distribution on the dispersion of the results can be clearly appreciated. As is expected, when the number of reeling cycles increases, the maximum tolerable defect decreases due to the low cycle fatigue. When the survival probability increases, the tolerable defect sizes are smaller.

7. SUMMARY AND CONCLUSIONS

An analytical model was proposed to determine CTOD as functions of strain history. Agreement between predicted and experimentally determined CTOD values is very good.

A "Material Memory" R curve approach seems to be adequate. End of second cycle CTOD values fell on single cycle R curve when plotted against total crack extension.

The total amount of crack extension after two cycles seems to be completely accounted for by the R curve, without fatigue effects.

If more reeling cycles are applied, fatigue effects need to be considered. Crack extension during multiple plastic strain cycles was modeled based on a fatigue formulation. Under elastic-plastic conditions, fatigue crack growth was described by the use of the cyclic J-integral range (ΔJ) as driving force. Closure effect was taken into account. Closure assumes that during a part of the load cycle the crack's surfaces come into contact and the crack closes. In this stage the specimen behaves as an uncracked body and consequently there is no crack growth.

A probabilistic fracture mechanics procedure for performing the structural reliability analysis of welded pipes subjected to multiple reeling cycles was developed. This procedure was based on a stable tearing fracture mechanics approach, a fatigue formulation and the Monte Carlo method.

A self-contained software tool containing this procedure was developed. The software allows assigning distributions for the material properties, geometry and the applied strain. The main program's outputs are the statistical distribution of critical crack size and the cumulative probability of failure for a given crack size.

The procedure was applied to a test case. Calculations were performed for several a/c aspect ratios and different number of reeling cycles. Tolerable defect size curves were obtained.

The results, obtained by this probabilistic approach permits a more realistic selection of maximum tolerable defect size than that provided by current standards and recommended practices.

REFERENCES

- [1] ASTM E1820, 1999, "Standard Test Method for Measurement of Fracture Toughness".
- [2] V. Kumar, M. D. German, C. F. Shih, "An Engineering Approach for Elastic-Plastic Fracture Analysis", General Electric Company, 1981.
- [3] Paris, P. C., Tada, H., Zahoor, A. and Ernst, H. A., "The Theory of Instability of the Tearing Mode of Elastic-Plastic Fracture, Elastic-Plastic Fracture", ASTM STP 668, American Society for Testing and Materials, Philadelphia, Pa., pp. 5-36, 1979.
- [4] Paris, P. C., Tada, H., Ernst, H. A. and Zahoor, A., "Initial Experimental Investigation of Tearing Instability Theory, Elastic-Plastic Fracture", ASTM STP 668, American Society for Testing and Materials, Philadelphia, Pa., pp. 251-265, 1979.
- [5] Ernst, H. A., Paris, P. C., and Landes J. D., "Estimation on J-Integral and Tearing Modulus T from a Single Specimen Test Record", Fracture Mechanics: Thirteenth Conference, ASTM STP 743, American Society for Testing and Materials, Philadelphia, Pa., pp. 476-502, 1981.
- [6] S. Wästberg, H. Pisarski, B. Nyhus, "Guidelines for Engineering Critical Assessments for Pipeline Installation Methods Introducing Cyclic Plastic Strain", Paper No. 51061, OMAE2004.
- [7] British Standard BS 7910: 1999, "Guide For Assessing the Acceptability of Flaws in Metallic Structures".
- [8] Offshore Standard DNV-OS-F101, "Submarine Pipeline Systems", 2000
- [9] Recommended Practice DNV-F108 "Fracture Control for Installation Methods Introducing Cyclic Plastic Strain", 2006.
- [10] H. A. Ernst, R. Bravo F. Daguerre and A. Izquierdo, "Strain History Effects on Fracture Mechanics Parameters. Application to Reeling", Paper No. 67007, OMAE 2005.
- [11] Rice, J.R., "Mechanics of Crack Tip Deformation and Extension by Fatigue", ASTM STP 415, American Society for Testing and Materials, Philadelphia, 1967, pp. 247-309.
- [12] H. A. Ernst, D. Passarella, R. Bravo and F. Daguerre, "Structural Reliability Analysis of Pipes Subjected to Multiple Strain Cycles – Application to Reeling Process", Paper No. 92473, OMAE 2006.
- [13] Dowling N. E. and Begley J. A., "Fatigue Crack Growth During Gross Plasticity and the J-integral", ASTM STP 590, 1976, pp 82-103.
- [14] T. Anderson, "Fracture Mechanics: Fundamentals and Applications", 2nd Edition, CRC Press, 1995.

- [15] R. C. McClung, G. G. Chell, Y. D. Lee, D. A. Russell and G. E. Orient, "Development of a Practical Methodology for Elastic-Plastic and Fully Plastic Fatigue Crack Growth", NASA/CR-1999-209428, July 1999.
- [16] SwRI, SES, Technip, Joint Industry Project "Validation of a Methodology for Assessing Defect Tolerance of Welded Reeled Risers".
- [17] H. A. Ernst, R. Schifini, R. Bravo, D. Passarella, F. Daguerre and M. Tivelli, "Probabilistic Fracture Mechanics Structural Reliability Analysis of Reeled Pipes", Paper No. 92474, OMAE 2006.
- [18] British Standard BS 7448: Part 4: 1997, "Fracture Mechanics Toughness Tests".
- [19] J. Lemaitre and J. Chaboche, "Mechanics of Solid Materials", 1994.
- [20] C.L. Xie, S. Ghosh and M. Groeber, "Modeling Cyclic Deformation of HSLA Steels using Crystal Plasticity". Journal of Engineering Materials and Technology, Vol. 126, No. 4: 339-352, 2004.

APPENDIX 1

Evolution of Stress – Strain Relationship

Constitutive equation for monotonically increasing load:

$$\frac{\varepsilon}{\varepsilon_0} = f(\sigma / Y)$$

Ramberg Osgood:

$$\frac{\varepsilon}{\varepsilon_0} = \frac{\sigma}{Y} + \alpha \left(\frac{\sigma}{Y} \right)^n$$

Cyclic loading [19, 20]:

If load reversal take place at $(\sigma_{ref}, \varepsilon_{ref})$ the subsequent (σ, ε) relationship is given by:

$$\frac{|\varepsilon - \varepsilon_{ref}|}{2\varepsilon_0} = f\left(\frac{\sigma - \sigma_{ref}}{2Y}\right)$$

Specifically, using Ramberg Osgood, the following equation is obtained:

$$\frac{|\varepsilon - \varepsilon_{ref}|}{2\varepsilon_0} = \frac{|\sigma - \sigma_{ref}|}{2Y} + \alpha \left(\frac{|\sigma - \sigma_{ref}|}{2Y} \right)^n$$

For load reversal: increasing load up to $(\sigma_{ref1}, \varepsilon_{ref1})$ + decreasing load, i.e. $\sigma < \sigma_{ref1}$:

$$\frac{\varepsilon_{ref1} - \varepsilon}{2\varepsilon_0} = \frac{\sigma_{ref1} - \sigma}{2Y} + \alpha \left(\frac{\sigma_{ref1} - \sigma}{2Y} \right)^n$$

For load reversal: decreasing load up to $(\sigma_{ref2}, \varepsilon_{ref2})$ + increasing load, i.e. $\sigma > \sigma_{ref2}$:

$$\frac{\varepsilon - \varepsilon_{ref2}}{2\varepsilon_0} = \frac{\sigma - \sigma_{ref2}}{2Y} + \alpha \left(\frac{\sigma - \sigma_{ref2}}{2Y} \right)^n$$

APPENDIX 2

Opening Load Calculation

$$\frac{\sigma_{op}}{\sigma_{max}} = A_0 + A_1.R + A_2.R^2 + A_3.R^3 \quad \text{for } R > 0$$

$$\frac{\sigma_{op}}{\sigma_{max}} = A_0 + A_1.R \quad \text{for } -2 < R < 0$$

When $\sigma_{op} > \sigma_{min}$, the coefficients are:

$$A_0 = \left(0.825 - 0.34\alpha_c + 0.05\alpha_c^2\right) \left[\cos\left(\frac{\pi\sigma_{max}}{2\sigma_{flow}}\right) \right]^{1/\alpha_c}$$

$$A_1 = (0.415 - 0.071\alpha_c) \cdot \frac{\sigma_{max}}{\sigma_{flow}}$$

$$A_2 = 1 - A_0 - A_1 - A_3$$

$$A_3 = 2A_0 + A_1 - 1$$

Where,

α_c , is the crack-tip constraint ($\alpha_c = 1.0$ for pure plane stress, or $\alpha_c = 3.0$ for pure plane strain)
 σ_{flow} = Flow stress ($[Y+T]/2$)